



On the Question of Predicting Deformations in the Vicinity of a Deep Quarry in a Tectonically Stressed Rock Mass

Gulnur Abdikarimova,¹ Lyazzat Shamganova,^{1,*} Nagimapanu Berdinova,¹ Zhansaya Lakhbayeva² and Svetlana Sedina¹

Abstract

One of the key safety concerns at the Kachar open-pit mine – currently exceeding 500 meters in depth – is the management of unstable slopes caused by stress-induced effects. High horizontal compressive stresses in the rock mass have a complex influence on slope stability. To analyze slope behavior as mining progresses toward the projected depth of 760 meters, a comprehensive methodology combining numerical modeling and geodetic monitoring was adopted. This integrated approach leveraged advanced software tools, accurate geomechanical characteristics of the rocks, and a robust representation of the stress-strain state. The principal stresses σ_1 and σ_3 derived from numerical simulations closely matched field measurements, providing confidence in the model's validity. Results from in-situ geophysical stress tests confirmed the reliability of the simulation outputs. The dominant failure mode identified was tensile fracturing, initiated by microcrack accumulation that leads to extensive delamination of the rock mass. This insight underscores the need for proactive stability management. The proposed predictive framework offers a dependable geomechanical assessment tool for tracking stress and deformation dynamics in the near-slope zone throughout different phases of mine development. By capturing both physical measurements and simulated behavior, it enhances safety planning and supports informed decision-making.

Keywords: Quarry; Stability; Geodynamic movements; Numerical model; Stress distribution.

Received: 18 June 2025; Revised: 21 September 2025; Accepted: 22 September 2025

Article type: Research article.

1. Introduction

At present, there is a long-felt need to take into account the actual stress-strain state when developing deeper horizons of solid mineral deposits. In highly stressed, solid and brittle rocks, displacements can be difficult to detect, right up to the moment of collapse. The main complication associated with the increase in mining depth is the increased risk of large-scale destruction of mining structures (pit walls and benches, mine workings and stope) caused by the action of tectonic stress fields, which is confirmed by periodically occurring powerful destructions at mines.

The existing approaches to its solution result in distinguishing two main groups of methods – direct and

indirect.^[1-2] The first group includes the methods based on measurements of rock deformation parameters. The second group includes geophysical methods that use variations of natural or artificially induced geophysical fields.

High horizontal stresses and increased depth can lead to unfavorable stress conditions, causing disintegration of rock mass and strength loss. These conditions cannot be satisfactorily taken into account by traditional stability analysis using the limit equilibrium method.^[3-4]

The problem of predicting the tectonic influence on the stress state of a rock mass is urgent in geomechanics. The initial stress state changes as the quarry is developed. The mined-out space in the rock mass causes the stress to be redistributed around the quarry. The resulting main stresses around the quarry have different directions compared to the initial stress state. Knowing the patterns of stress distribution in rocks ensures safe and efficient operation of deposits in a range of mining, geological and mining engineering conditions.^[5]

Characteristic features of tectonically stressed rock masses are specific manifestations of rock pressure in

¹Branch of the Republican State Enterprise "National center for complex processing of mineral raw materials of the Republic of Kazakhstan" D.A. Kunayev Mining Institute, Almaty, 050046, Kazakhstan

²Department of Chemistry, Faculty of Natural Sciences and Geography, Abai Kazakh National Pedagogical University, 30, Kazybek bi, Almaty, 05001, Kazakhstan

*Email: l.shamganova@gmail.com (Lyazzat Shamganova)

underground workings, core diskings and azimuthal deviations of borehole shafts as well as abnormally high values of stress field components in one of the horizontal (or close to it) directions.^[6-9]

There are still no developed theoretical methods for analyzing the tectonic stress state of a rock mass.

Many works deal with the problems of formation of stress-strain state. One of the first researchers to put forward a hypothesis about the causes of stress-strain state of rock masses was the Swiss geologist A. Heim. Based on observations of a rock mass behavior during the excavation of a large transalpine tunnel back in the 1970s, he concluded that the rock is in a spatial stress state. In this case, the vertical component of the stress is equal to the weight of the overlying rocks. The main point of Heim's hypothesis^[10] was that the stresses are of geological origin, and the ratio of the vertical and horizontal components is close to one (hydrostatic stress distribution).

Numerous experimental data obtained in recent decades have shown that in many cases the ratio in real rock masses did not correspond to the stress measurements. Based on a large number of stress measurements in deep mines in Scandinavia, the Swedish geologist N. Hast^[11] established that horizontal stresses are often greater than vertical ones. The same conclusion was reached by American researchers Barry Voigt, J. Taylor, J. Voigt and G. Herget^[12] as well as Hiromatsu and Oka.^[13]

The depth of excavation related damage induced by high stress concentrations in brittle rock masses has relied on empirical methods (for example, Martin *et al.*, 1999, Diederichs, 2007) or case specific numerical modelling (for example, Hou, 2003, Hudson *et al.*, 2009, Rutqvist *et al.*, 2009, Lisjak *et al.*, 2015a, Lisjak *et al.*, 2015b).^[14-17]

Well known are the works of a group of researchers led by J. Sjöberg, who is engaged in a range of issues related to the stability of the Aitik quarry (Sweden). In this quarry, despite the rather fractured and watered rock mass, it was possible to form a final pit wall with a slope angle of 51°.^[18-19]

It is worth noting the studies conducted under the supervision of A. Karzulovic. These studies are based, as a rule, on a fairly detailed description of the lithological features of the rocks that make up the studied pit walls. The quarry field is divided into sections that can be considered homogeneous in their geological structure. Further recommendations on the stability of quarry walls are given for each section.^[20] It is also essential to emphasize that the stress-strain state of rocks cannot be separated from their mineralogical and chemical composition. The breakdown of silicate lattices, hydration-dehydration reactions of clay minerals, and oxidation-

reduction processes within sulfide ores can significantly influence the strength and long-term stability of rock masses under deep mining conditions. For example, pyrite oxidation in fractured zones leads to the formation of sulfuric acid, which accelerates the dissolution of carbonates and weakens cementing bonds between mineral grains. Similarly, hydration of feldspars and micas produces swelling clays that reduce shear strength, while pressure-induced phase transitions of quartz and feldspar at great depths alter the elastic modulus of the rock. These chemically driven transformations act in synergy with mechanical stresses, enhancing fracture propagation and destabilization. Therefore, in addition to geomechanical and geophysical models, an adequate evaluation of quarry wall stability at great depths requires consideration of geochemical reactions, mineral stability fields, and thermodynamic properties of rock-forming compounds.

To date, the works related to the study of structural and geological features of rock masses, including for the purpose of determining stable slope angles in quarries, are based on various indicators of rock mass quality (ratings).^[21-28] It can be noted that none of the known systems for assessing the quality of a rock mass fully takes into account its stress-strain state.^[29] Opencast mining in tectonically stressed rock masses, accompanied by an increase in the level of both gravitational and tectonic active stresses, inevitably results in a situation when rock masses begin to collapse in a dynamic mode.^[30]

The combination of tensile damage and decrease in confinement play an important role in stress-induced failure of hard rocks at great depths. Extensile fracturing at low confining stresses encountered at and close to the excavation boundary occurs as a result of exceeding the rock mass strength controlled by damage initiation mechanisms that are relatively insensitive to confinement and by fracture propagation mechanisms that govern the rock mass response at low confining stresses.

Massive to moderately jointed rock masses with a high ratio of compressive to tensile strength under anisotropic, high-magnitude stress regimes are prone to brittle fracturing, with the dominant failure mechanism being that of extensile fracturing, as previously mentioned.^[31]

Vazaios and colleagues demonstrated that the Finite-Discrete Element Method (FDEM) is capable of accurately simulating tensile fracturing and brittle failure that occur in hard rocks under high-stress conditions during their extraction.^[32]

Various researchers have utilised different numerical methods in order to assess brittle fracturing in rock mass excavations, varying from the application of continuum

techniques^[31,33] to discontinuum, and hybrid finite-discrete element approaches.^[34,35]

This occurs when the deformation of the rock reaches a critical value, which leads to its destruction.^[36-39] In this case, to assess the stability of the rock mass, the level of the acting stresses is calculated for the design depth of the quarry. Numerical methods for calculating the distribution of stresses are used for this. At the same time, the stability of the walls is assessed based on a comparison of the level of the estimated stresses in the vicinity of the wall against the ultimate strength of the rocks. If the level of the estimated stresses in the designed structure does not exceed the ultimate strength of the rocks with due account for the safety factor, then in this case the structure is considered generally stable.

The management of unstable walls caused by the action of the stress-strain state is one of the most important issues in solving safety issues in the Kachar quarry, the actual depth of which currently exceeds 500 m. At the Kachar quarry, an unforeseen deformation process caused by a change in the stress-strain state of the rock mass under the action of geodynamic movements resulted in significant destruction and suspension of quarry operations in 2015 and economic losses. The stress-strain state of the Kachar quarry is of the gravitational-tectonic type with a fairly high level of horizontal compressive stresses. For deep quarries, the stress state is much more complex due to zones of both low and high stresses.

The Kachar deposit is characterized by complex engineering-geological and hydrogeological conditions of occurrence. Long periods of open-pit mining and the associated large volumes of rock mass movement contributed to the disruption of the natural stress-strain state of the earth's crust in the area of the deposit.

Landslide-type processes are typically observed only in the uppermost benches of the pit and are most commonly triggered during periods of seasonal flooding. At the benches located at the ± 0 m level and below, instances of rapid bench collapses extending over several meters have been recorded. These failures are most often associated with the presence of slip planes within the rock mass. Deformation processes are unevenly distributed across the pit area, with the highest concentration of events observed on the southwestern and northeastern pit walls. The deformation processes occurring in the area of the crushing and conveying complex, which began in 2011, were a consequence of rock mass failure caused by a high level of horizontal tangential stresses induced by ongoing geodynamic movements of the Earth's crust.

The stress state and its parameters acting in the horizontal plane plays an ambiguous role. At moderate levels, they

contribute to increased stability compared to the calculated values. However, when certain thresholds are exceeded, they cause disturbances in the form of shear fractures that propagate deep into the pit wall. The rock mass bounded by these fractures undergoes failure. Our analysis suggests that in moderately fractured rock masses under anisotropic stress conditions, failure predominantly initiates with the formation of tensile fractures. This mechanism triggers the accumulation of microcracks, which, as they develop, lead to large-scale fracturing, ultimately resulting in rock failure or delamination. To analyze the stability of the Kachar walls when it was deepened to 760 m, an integrated approach was used, combining numerical modeling methods and field studies that took into account the stresses acting in the rock mass.^[40-45]

This study aims to improve understanding and prediction of the stress-strain state in deep open-pit mining by analyzing geodynamic movements at the Kachar quarry, determining geological and structural factors affecting rock stability, creating a 3D numerical stress distribution model, applying mechanical failure criteria to assess brittle fracturing, evaluating pit wall and bench stability with increasing depth, integrating field monitoring with modeling to forecast hazardous zones, and proposing measures for safe and sustainable quarry operation under complex tectonic and geomechanical conditions.

2. Methods and materials

2.1 Analysis of recent geodynamic movements at the kachar quarry

The Kachar quarry is located in the Kostanay Region of northern Kazakhstan.

The geotechnical conditions for the development of the Kachar iron ore deposit are very complex and are determined by:

- the presence of a 130÷200m layer of loose sediments;
- the 30°-60° dip of sedimentary rock bedding towards the mined-out space typical of the northwestern, western, southwestern and southern walls, and the presence of weakened surfaces along the bedding;
- the presence of karsting, watered limestones in the structure of the western, southwestern and southern pit walls. The limestones in the southern part of the quarry are especially watered;
- the presence of faults and zones of excessive fracturing in the Paleozoic rocks;
- the presence of five aquifers;
- the intensive manifestation of recent geodynamic activity of natural and man-made genesis.

Structural disturbances of various scales have been identified along almost the entire perimeter of the pit. The southwestern part of the pit is the most heavily disturbed, where four zones of major disrupted blocks have been

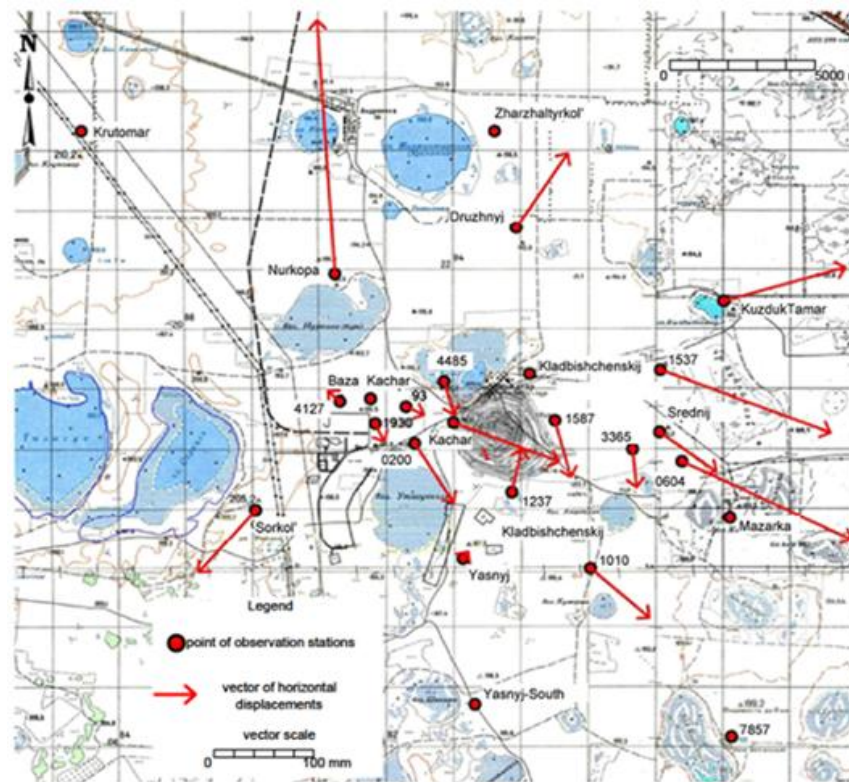


Fig. 1: The vectors of horizontal geodynamic displacements of geodetic points in the area of the Kachar quarry.

delineated.

The parameters of the stress-strain state of the rock masses of the Kachar quarry were determined using geodetic methods by means of redefining the coordinates of geodetic points in adjacent territories using satellite geodesy technologies.^[46-49]

At each point, located both within the deposit and away from it, cyclic measurements of spatial coordinates were performed using the satellite positioning method. As a result of office analysis of the measurement results and mathematical analysis, displacements of the geodetic network points were determined.

The vectors of horizontal displacements of geodetic points characterizing the recent geodynamic movements in the quarry and the corresponding stress-strain state (Fig. 1).

Cyclic short-term movements include displacements that take place once or several times during continuous several-hour observation sessions.^[50-54]

The parameters of cyclic short-term geodynamic movements are determined by means of continuous several-hour monitoring of the benchmark system by satellite methods. The measurements record changes in the spatial coordinates of the monitoring network points. The interval between discrete measurements can vary from several minutes to several tens of minutes. The continuous monitoring by satellite geodesy complexes ensures the obtainment of all three coordinates of the device's location at a given time. The use of

several devices simultaneously results in the obtainment of a spatial displacement of the points, where the devices are located, relative to each other at any given time interval (from several tens of minutes to several hours). The accuracy of displacement measurements between points is 1-5 mm.

Using the mathematical methods of continuum mechanics, the deformations of intervals, the values and directions of displacement vectors obtained as a result of instrumental observations were transformed into a tensor representation of the deformation field with the identification of the main components of the deformation tensor.

In line with the research results, within the studied rock mass of the Kachar quarry, two structural blocks are distinguished that have oppositely directed mutually perpendicular recent geodynamic movements – northwestern and southern. The displacement of the northwestern block to the south creates a zone of concentration of compressive stresses and deformations in the contact area of structural blocks in the southwestern pit wall. This can cause shear cracks in the rock mass of the wall along with the disruption of the primary structure and destruction of the shifted rock mass. The boundary of the zone of compression and tensile deformations goes along the tectonic fault in the north-eastern direction (Fig. 2). The values of vertical displacements in the quarry area during its existence have been in the range from +0.391 m to -0.209 m. Surface subsidence gradually increases

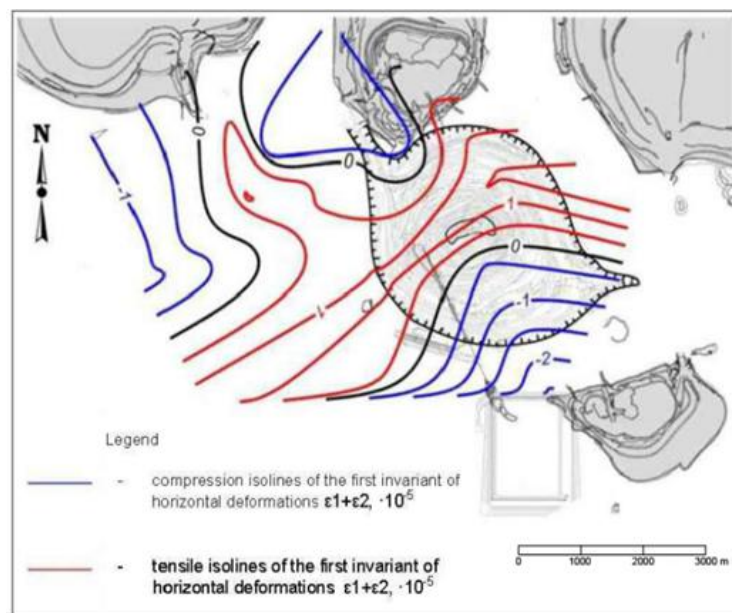


Fig. 2: The distribution of isolines of the first invariant of horizontal deformations in the area of the Kachar quarry.

from the western pit wall in all directions.

The vectors of horizontal movements of points are generally multidirectional and have rather small values from 0.003 m to 0.025 m.

The initial and secondary stress-strain states of adjacent rock masses of the Kachar quarry are very heterogeneous, which leads to micro-movements of large geological blocks along tectonic contacts, and can cause changes in the hydrogeomechanical structure of the adjacent rock mass and the groundwater regime. In harmony with the parameters of recent displacements of peripheral geodetic points, their values and directions, the initial stress-strain state in the quarry area as a whole is formed under the influence of tensile deformations.

The analysis of the obtained results shows that the western slope of the quarry exhibits more heterogeneous deformation characteristics compared to the other slopes. This area contains zones of increased tensile and compressive concentrations that alternate with each other. Elevated values of tensile deformations are observed on the eastern slope of the quarry, while a slightly increased concentration of compressive deformations is present on the northeastern slope.

The formation of the anomalous zone with high compressive tangential stresses, which caused shear failures at the -30 m level of the Kachar quarry in 2015, was due to the mutually perpendicular displacements of adjacent structural blocks under the influence of ongoing geodynamic movements.^[55]

2.2 Numerical modeling of the stress state of the rock mass of the kachar quarry

A three-dimensional model of the Kachar quarry was built in the Datamine software (Fig. 3). Almost all the rocks that make up the adjacent rock mass of the Kachar quarry are brittle. Numerical models help in assessing failure mechanisms, stress distribution, energy changes, and deformation changes, among several other factors which influence the stability of deep mining excavations.^[56] The estimated physical and mechanical properties of the identified lithotypes of the quarry rock mass obtained in the course of various studies are presented in Table 1.

The numerical modeling was performed using the RS2 RocScience software,^[57] where the slope stability was quantitatively assessed using the shear strength reduction method (SSR).

The entire simulation model of the pit wall down to the design depth of 760 m (level -570 m) was divided into many finite elements based on lithological differences, connected to each other at the vertices, which were then assigned their physical and mechanical characteristics.

The model was controlled by boundary conditions – along the lateral boundaries and at the base of the model, all nodes were assigned fixed boundary conditions (prohibition of displacements). The surface of the estimated area remains free for deformations and displacements.

The maximum component of the initial stress state of the rock mass is modeled subparallel to the strike of the ore deposit. The stresses and their change with increasing depth are assessed in-situ on the basis of regional stress values. The coefficients of lateral soil pressure in two opposite directions of the main stresses were $\lambda_1=2.03$ and $\lambda_2=1.31$.

To model the nature of rock deformation at the Kachar

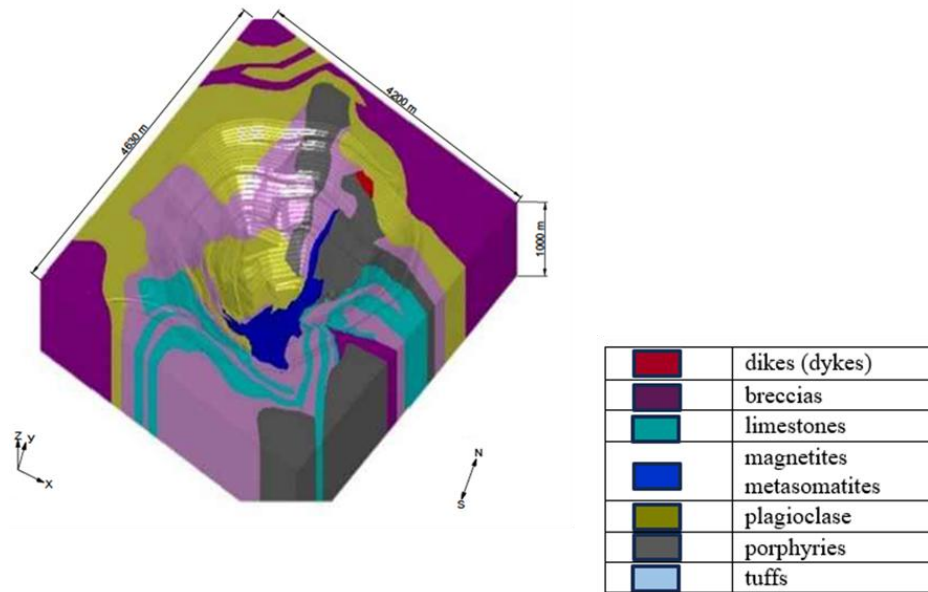


Fig. 3: The geometry of a three-dimensional numerical model for modeling the stress-strain state.

Table 1: Physical and mechanical characteristics of rocks taken into account during the modeling.

Rock Type	σ_{ci} (MPa)	GSI	mi	Em (MPa)	ν	σ_t (MPa)	C (MPa)	φ
OVERBURDEN ROCK	-	-	-	-	-	0	0.040	17
FAULT	20	30	6.6	0.3	0.34	0	0.010	22
WEATH	0.7	40	6	0.3	0.34	-	0.010	22
BRX	26	61	12.5	25.24	0.23	5.1	1.652	36.4
LST	67	71	12.9	55.55	0.25	5.3	3.214	45.9
META	64	71	9.9	33.31	0.23	7.2	2.537	40.8
ORE	33	63	16.7	10.20	0.21	7.4	2.625	37.2
PLAG	71	63	16	5.08	0.27	6.7	1.085	42.1
TUFF	72	62	17.5	35.74	0.23	7.9	2.801	46.6
Rock Type	σ_{ci} (MPa)	GSI	mi	Em (MPa)	ν	σ_t (MPa)	C (MPa)	φ

where: σ_c = uniaxial compressive strength of intact rock, GSI = the geological strength index, m_i = Hoek-Brown dimensionless material constant for intact rock, E_{rm} = Young's modulus of rock mass, ν = Poisson's ratio, σ_t = tensile strength, C = cohesion, φ = internal friction angle.

quarry, the Mohr-Coulomb elastic-plastic medium model was used. This criterion serves to describe the response to shear stress and normal stress by materials.^[58-60]

Brittle failure is caused by the excess of the greatest normal stress over the rock ultimate compressive or tensile strength. Shear fracture is characterized by significant tangential stresses exceeding the ultimate shear strength of rocks (this type of failure is always preceded by the development of noticeable plastic (inelastic) deformations).

The maximum normal stress theory (the maximum-stress theory) is based on a comparison of the latter with the

compressive and tensile strength of rocks, taking into account the disturbance of the rock mass presented in Eq. (1):

$$\begin{aligned} \sigma_1 &\leq K_C \sigma_{ci} \\ |\sigma_3| &\leq K_C \sigma_t \end{aligned} \tag{1}$$

where σ_1 and σ_3 are respectively, the maximum compressive and minimum tensile principal stresses acting in the rock mass (obtained from the elastic solution), MPa; K_C is the coefficient of structural weakening; σ_{ci} is the ultimate compressive strength of the rock, MPa; σ_t is the ultimate tensile strength of the rock, MPa.

In real conditions, the rock mass is characterized by cracks. Therefore, possible risks in the calculations of the stability indicator were taken into account through the coefficient of structural weakening of the rock mass ($K_C = 0,5$).

According to Protodyakonov’s research,^[61] it has been established that the rock strength is influenced only by the ratio of maximum and minimum stresses (σ_1, σ_3), in the plane of which the maximum shear stress acts (τ_{xy}).

In accordance with the strength theories for brittle materials,^[62] in practice it is considered that the loss of stability of a section of the adjacent rock mass, according to the results of numerical modeling, is possible when one of the following criteria is realized:^[56-57]

- when the maximum component of compressive stresses σ_1 exceeds 50% of the ultimate uniaxial compression strength of rocks (σ_{ci}) that make up the wall section ($|\sigma_1| \geq 0.5 |\sigma_{ci}|$), the rock mass enters the limit state;
- when the minimum component of tensile stresses σ_3 exceeds the ultimate tensile strength: $\sigma_3 > \sigma_t$, opening of natural cracks and formation of man-made cracks is possible;
- when the maximum tangential stresses τ_{xy} exceed the ultimate shear strength, there is a possibility of shift of rock blocks along natural and man-made cracks.

According to the theory of limit equilibrium, the condition of stability (non-failure) under biaxial stress for an arbitrary plane, such as along I-I (Fig. 4), is determined by an inequality that relates the normal and shear stresses based on the Coulomb failure criterion Eq. (2):^[63]

$$\tau_{xy} < [\tau_0] + \sigma_n tg\varphi \tag{2}$$

where

τ_{xy} is effective maximum shear stresses;

C, φ are adhesion and angle of internal friction of the destroyed material;

σ_n is a normal component of stress acting on the sliding surface.

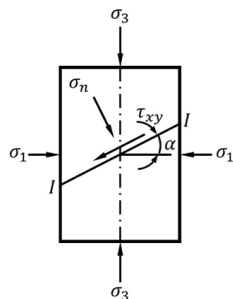


Fig. 4: Stress distribution diagram on a plane during failure in the form of spalling (shear).

In shear failure according to the Mohr–Coulomb criterion,

the interaction between normal and shear stresses, as well as the material’s internal properties (cohesion and internal friction angle), determine the onset and plane of failure.

The stress components on an arbitrary plane can now be expressed in terms of the principal stresses as shown in Eq. (3) and Eq. (4):

$$\sigma_n = \sigma_3 \cos^2 \alpha + \sigma_1 \sin^2 \alpha \tag{3}$$

$$\tau_{xy} = \frac{\sigma_1 - \sigma_3}{2} \sin 2\alpha \tag{4}$$

where σ_1 and σ_3 are maximum and minimum principal stresses respectively; α is the angle of inclination of the sliding surface to the line of action of the minimum principal stress σ_3 .

Shear stresses reach their maximum values on planes oriented at an angle of 45° to the principal planes.

The general condition for the loss of stability of an individual bench is the exceeding of resisting forces by the acting shear forces.

Based on this, and using formulas (2), the factor of safety with respect to the maximum shear stress τ_{max} can be calculated using the following expression for $\alpha = 45^\circ$ Eq. (5):

$$n = \frac{(\sigma_1 + \sigma_3)tg\varphi + 2C}{2\tau_{xy}} \tag{5}$$

where

φ is the angle of internal friction, degree

C is adhesion in the rock mass, t/m^2

3. Results and discussion

The stress-strain state of the host rocks of the Kachar quarry was assessed in two of the most characteristic perpendicular sections: in the direction of the northwest-southeast walls (across the strike of the ore body).

Letter designations of the main stresses according to their values, as used in calculations:

σ_1 –major principal stress at failure

σ_2 – the principal intermediate stress

σ_3 –minor principal stress at failure

τ_{xy} – the maximum shear stress.

The Kachar open-pit mine is located approximately 45 km north of the city of Rudny, the nearest major population center.

By the end of its operational life, the Kachar pit will measure approximately 3 km by 2.5 km in diameter, with a current depth of about 450 meters (Fig. 5). The final planned depth of the pit is 750 meters.

The Kachar open-pit mine, with a present depth of ~450 m and projected depth of 750 m, represents one of the largest



Fig. 5: Kachar Open-Pit Mine (Google, 2023).

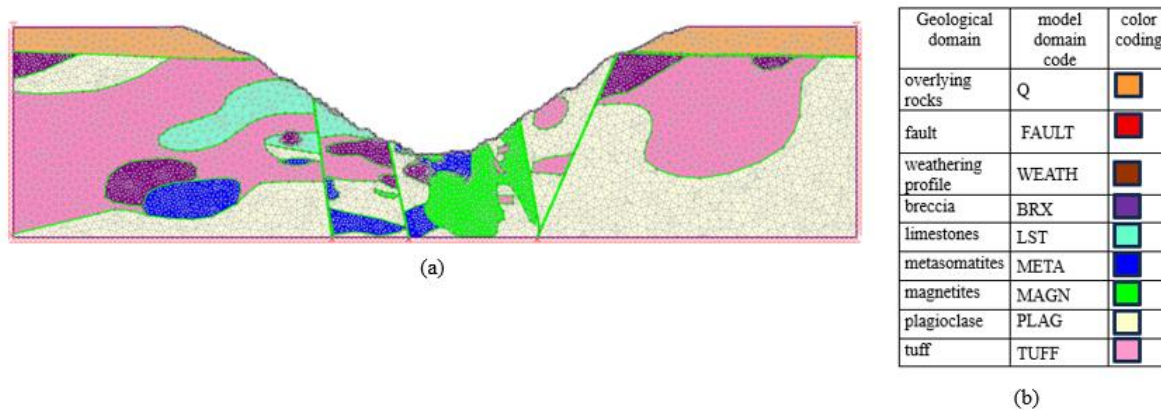


Fig. 6: a) Finite element model of the Kachar open-pit slope in the northwestern (NW) and southeastern (SE) directions after discretization and mesh generation b) lithology color coding.

iron ore excavations in northern Kazakhstan (Fig. 5). The pit geometry, approximately 3 km by 2.5 km, creates an immense zone of redistributed stresses within the host rock mass. Such large-scale excavation alters the natural gravitational–tectonic equilibrium of the crust, producing both compressive and tensile anomalies along pit slopes. Similar effects have been reported for other deep open-pits worldwide, such as the Palabora mine in South Africa and the Chuquicamata pit in Chile, where depth-induced stress anisotropy generated hazardous instabilities. [64-65] The combination of steep slope geometries and brittle lithologies creates conditions highly sensitive to geodynamic perturbations. The development of fractures, faults, and zones of stress concentration is

particularly pronounced in the northwestern (NW) wall, consistent with field evidence of recurrent deformations. This underscores the importance of combining geometrical analysis with advanced modeling and geodetic monitoring to capture the evolving stress–strain state.

Fig. 6 and 7 show the finite element model of the Kachar open-pit slope in the northwestern (NW) and southeastern (SE) directions after discretization and mesh generation, as well as the stress contour distribution, produced using the RS2 software by Rocscience.

The finite element model (FEM) constructed for the Kachar quarry (Fig. 6) discretizes the pit walls and adjacent rock mass into lithological blocks with distinct mechanical

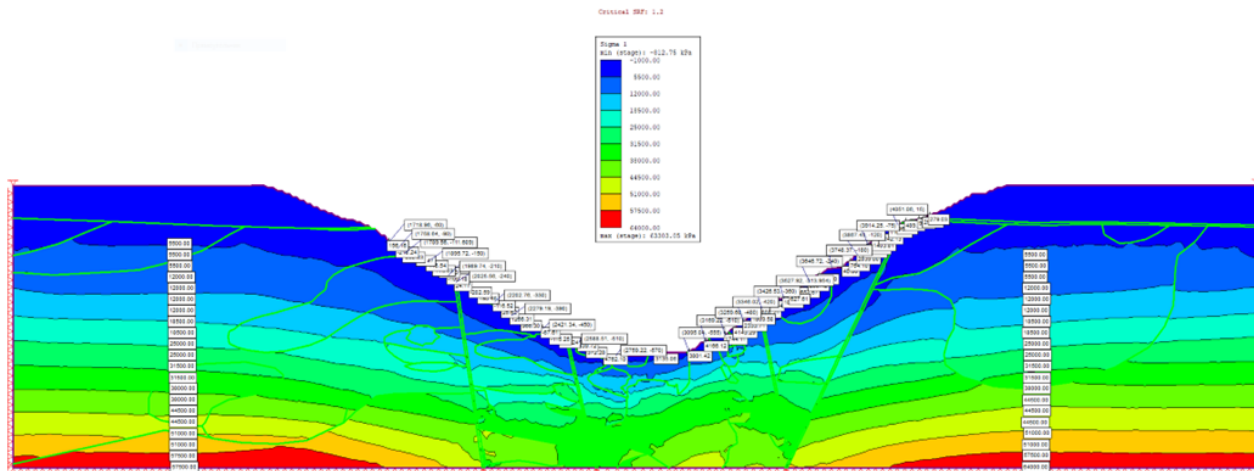


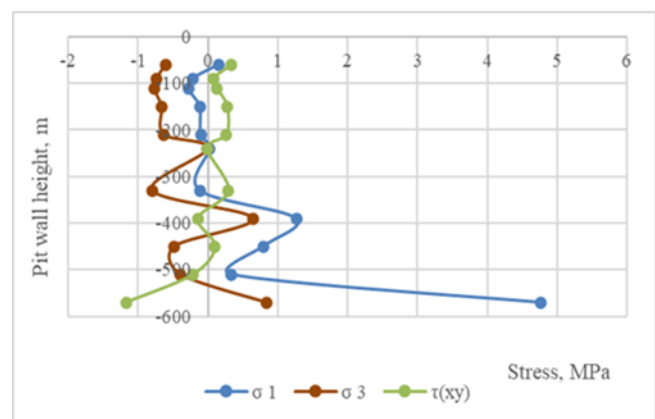
Fig. 7: Contour plot of the in-situ stress distribution.

properties (see Table 1). Such models have proven effective in simulating complex stress redistribution patterns in heterogeneous geological environments.^[55,66] The discretization ensures that contrasts between strong lithotypes (e.g., tuffs, limestones) and weaker units (fault gouge, weathered rock) are realistically represented. The adoption of the Mohr–Coulomb elastic–plastic criterion allows for simulation of shear-dominated failure, while tensile fracture initiation is captured through tensile stress thresholds. Importantly, the FEM accounts for anisotropy in lateral stress coefficients ($\lambda_1 = 2.03$, $\lambda_2 = 1.31$), which reflects the strong tectonic control over the stress regime. Comparable anisotropy has been noted in Scandinavian and Canadian deep mines, where horizontal stresses often exceed vertical stresses due to glacial and tectonic loading histories.^[67-68]

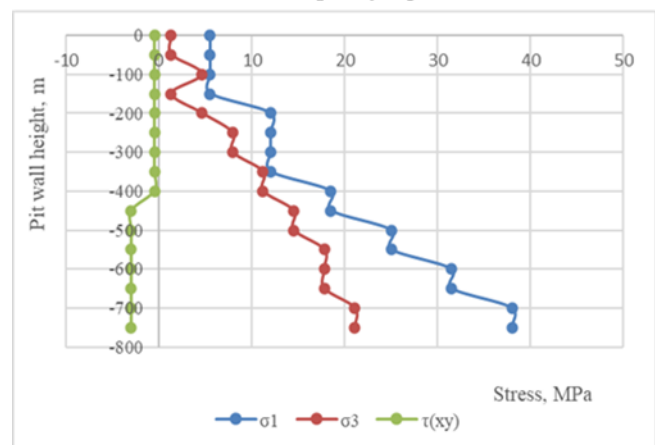
Fig. 8 presents the stress distribution graphs of the principal stresses σ_1 , σ_3 , and shear stress τ_{xy} along the northwest–southeast direction of the Kachar open-pit mine, for both the excavation area and the surrounding rock mass.

The stress contour plots (Fig. 7) demonstrate the non-uniform propagation of stresses within the quarry. Zones of elevated σ_1 (major principal stress) are concentrated near slope faces and lithological boundaries, especially where strong rock types are juxtaposed with weaker fault materials. This agrees with international observations that stress heterogeneity intensifies around geological discontinuities, which act as both stress concentrators and potential slip planes.^[69,15] Stress “shadow zones,” characterized by low σ_1 and σ_3 values, are also evident in the model. These regions can create instability “windows” by promoting differential displacement, eventually triggering localized collapses. In the Kachar quarry, these effects are magnified by hydrogeological activity, as water-bearing limestones and aquifers further reduce effective stress and accelerate chemical weakening of rocks through

dissolution and hydration processes.^[70]



(a) for quarrying.



(b) for rock mass.

Fig. 8: The distribution of σ_1 , σ_3 , and τ_{xy} with depth of the pit, based on simulation results for both the quarrying and the surrounding rock mass.

The stress profiles with depth (Fig. 8) reveal critical thresholds for instability development: Alternating tensile and compressive stress zones at -300 to -330 m; These stress

Table 2: Impact assessment of shear stresses τ_{xy} on the rock mass of the Kachar quarry in the direction of the northwest-southeast pit walls based on the results of numerical modeling.

Pit wall	Dangerous areas in terms of deformations, horizons m	Fulfillment of non-failure condition			Estimated safety factor of the section	Predicted condition of the section
		$\tau_{xy} < [c] + \sigma_n \tan \phi$	Effective maximum shear stresses τ_{xy} , MPa	Estimated ultimate shear strength, MPa		
NW	(-510) ÷ (-555)	1.54	1.46	0.94	Possible development of shear deformations	

reversals correspond to tectonic fault zones intersecting the NW wall. The alternation of stress regimes facilitates shear offset along pre-existing discontinuities, consistent with case histories of tectonically stressed pits in Chile and Sweden.^[71-72] Non-uniform σ_1 distribution near excavation boundaries; Elevated σ_1 values contribute to localized shear cracking and spalling, particularly at shallow to intermediate depths. Concentration of maximum shear stresses τ_{xy} at -510 to -555 m; The modeled τ_{xy} values reach 1.54 MPa, surpassing the ultimate shear resistance of plagioclase-rich zones (1.46 MPa, see Table 2). This exceeds the stability threshold, indicating the likelihood of shear slip or dynamic failure at these depths. Low confinement in the NW wall; The predominance of low σ_3 values fosters extensional fracturing, which aligns with field evidence of tensile failure being the dominant mode in Kachar. Similar findings were reported by Martin *et al.*^[68] and Kaiser *et al.*,^[73] who demonstrated that extensional spalling dominates in brittle, low-confinement conditions.

The analysis of distribution of the main σ_1 and σ_3 and maximum shear stresses τ_{xy} in the direction of the northwest-southeast walls of the Kachar quarry up to the (-570) m level based on the results of numerical modeling shows:

- at the levels of (-300) m – (-330) m of the northwestern pit wall of the Kachar quarry, the main stresses in the mass blocks change. Zones of tensile and compressive stresses alternate in the tectonic fault zone. The boundary of the zone of compressive and tensile deformations goes along the tectonic fault in the northeastern direction;
- the distribution pattern of the maximum stress component σ_1 for the quarrying of the northwestern wall is non-uniform. The maximum stress component σ_1 acting near the quarrying of the northwestern pit wall affects the configuration of the pit wall (contributes to the deformations in the form of shear cracks) up to the horizon (-330) m.;
- the greatest shear stresses in the northwestern wall (up to 1.54 MPa) are concentrated at the (-510) – (-555) m

horizons, at the intersection points of the slope with the bench toe. This section will be potentially dangerous in terms of dynamic fracture;

- according to the results of numerical modeling, the geomechanical state of the rock mass in the northwestern slope is characterized by low compressive stress.

For the most stressed section, where there is an unfavorable effect of shear stresses on the adjacent rock mass and the maximum shear stresses (τ_{max}) may exceed the ultimate shear strength (Table 2), the non-failure condition was checked according to (2) and the stability factor of the deformable section was calculated according to (5).

The values of the maximum shear stress component τ_{xy} in the marginal zone of the northwestern pit wall are concentrated at the (-510) ÷ (-555) m levels composed of plagioclases, and are equal to 1.54 MPa. The estimated stability factor of the section at the intersection points of the slope with the bench toe is 0.94. Here, the development of shear deformations is probable.

Table 2 presents a quantitative assessment of the NW wall stability at critical depths. The calculated stability factor of 0.94, below unity, confirms that the rock mass is at or beyond the threshold of shear failure. This result is consistent with the observed deformations in the NW sector of the quarry.

A safety factor <1.0 is unacceptable for long-term pit stability. International practice dictates that a factor of at least 1.2–1.5 is required for operational safety.^[20,74] Thus, the Kachar quarry’s NW wall, particularly between -510 and -555 m, represents a geomechanically unstable zone where preventive measures are urgently needed. These could include slope flattening, controlled destress blasting, drainage of water-bearing zones, or chemical stabilization of weak horizons.^[75]

The distribution of deformation processes over the quarry based on the data obtained from deformation data sheets (Fig. 9),^[43-45] The areas where deformation events are concentrated characterize the general stress-strain state of the Kachar rock mass. The northwestern section is characterized by the most

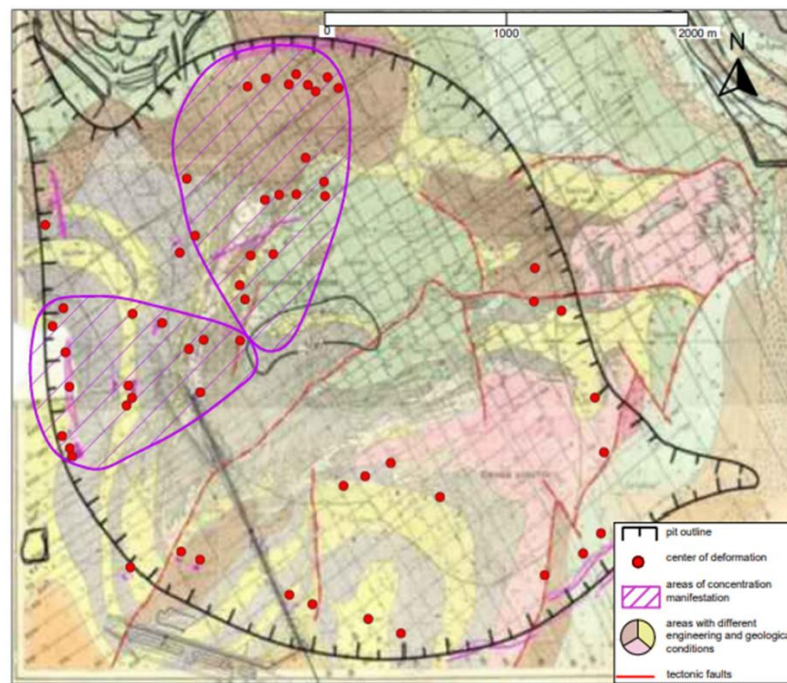


Fig. 9: Distribution of actual deformations over the quarry surface.

unfavorable mode of occurrence.

Due to the use of modern software tools, accounting for the geomechanical properties of rocks and a reliable representation of the stress-strain state model of the rock mass, the distribution of principal stresses σ_1 and σ_3 predicted by the numerical model agrees well with field observations and adequately reflects the real processes in the rock mass.

Numerical modeling enhances our understanding of the behavior of brittle rocks and provides well-founded predictions of the expected level of damage. Every mining operation must perform stress modeling as excavation progresses to avoid unforeseen problems during subsequent stages of development.

The distribution of actual deformations (Fig. 9) across the quarry surface validates the reliability of the numerical model. Deformation hot-spots coincide with zones of elevated stress predicted in Fig. (7–8), particularly in the NW wall. This congruence between modeled and observed behavior underscores the robustness of integrating numerical modeling with geodetic monitoring.

The field data show that deformation processes are not evenly distributed across the quarry:

NW wall: exhibits the highest concentration of deformation events, consistent with the lowest safety factor and highest τ_{xy} values.

Eastern slope: predominantly tensile deformation zones, reflecting extensional fracturing under low confinement.

Western slope: alternation of compressive and tensile zones, producing complex deformation signatures.

The distribution of deformation processes over the quarry based on the data obtained from deformation data sheets (Fig. 9).^[43] The areas where deformation events are concentrated characterize the general stress-strain state of the Kachar rock mass. The northwestern section is characterized by the most unfavorable mode of occurrence.

Due to the use of modern software tools, accounting for the geomechanical properties of rocks and a reliable representation of the stress-strain state model of the rock mass, the distribution of principal stresses σ_1 and σ_3 predicted by the numerical model agrees well with field observations and adequately reflects the real processes in the rock mass.

Chemical–Geomechanical Interactions in the Stress–Strain State: The results obtained clearly demonstrate that the Kachar quarry rock mass is highly sensitive not only to mechanical stress redistribution but also to chemical and mineralogical transformations. The lithological units present (limestones, plagioclase-rich rocks, tuffs, and sulfide ores) undergo physico-chemical processes under stress, fluid circulation, and exposure, which strongly influence stability.

In fractured sulfide-bearing zones, pyrite oxidation ($\text{FeS}_2 \rightarrow \text{Fe}^{2+} + \text{SO}_4^{2-}$) generates sulfuric acid, accelerating carbonate dissolution and weakening intergranular cementation. This chemical degradation reduces cohesion and magnifies the propagation of microcracks already predicted by stress analysis. Hydration of feldspars and sheet silicates further produces swelling clays, lowering shear strength—an effect consistent with observed collapses during seasonal flooding.

At greater depths, phase transitions of quartz and feldspars under pressure alter elastic moduli and influence the stress–strain response, shifting mechanical failure thresholds. Simultaneously, redox reactions involving Fe- and Mn-bearing minerals modify porosity and permeability, creating preferential weakness planes that often coincide with zones of concentrated shear stresses identified in the numerical models. These findings show that mechanical and chemical processes act in synergy, amplifying rock mass instability. For reliable forecasting, stress-strain modeling must be integrated with geochemical stability fields and thermodynamic simulations of mineral reactions. Such an approach would enable the identification of chemically active hazard zones where dissolution, hydration, and oxidation overlap with mechanically critical stress regimes.

In the Kachar quarry, high-risk zones are anticipated along tectonic contacts, karstified limestones, and sulfide-rich ore horizons. Similar to the way phytoremediation studies have demonstrated the importance of understanding geochemical interactions and their effects on plant physiology,^[76] effective slope management in deep mining also requires a multidisciplinary approach. In this context, an integrated monitoring system that combines geodesy, hydrochemistry, mineralogy, and numerical geomechanics is essential for assessing and mitigating geotechnical hazards. Such agreement between field and numerical evidence reflects best practice in geomechanics, where model calibration against monitoring data enhances predictive capability.^[77]

The findings of this study carry several important implications for the broader field of deep open-pit mining and geomechanics. First, the results confirm that tensile fracturing under conditions of low confinement constitutes the dominant failure mechanism at the Kachar quarry. This observation is consistent with the established theory of brittle failure in hard rocks, whereby the progressive accumulation of microcracks under tensile loading evolves into large-scale macrofracturing and eventual delamination of the rock mass.^[15,73]

Second, the study demonstrates that the most critical stress conditions are concentrated at depths of –510 to –555 m. This depth interval represents a key hazard zone, as further mining towards the projected depth of 750 m is expected to amplify the extent of deformation. Without appropriate reinforcement measures, progressive failure originating in this zone could propagate both upwards and laterally, thereby threatening the stability of benches, pit walls, and haulage infrastructure.

Third, the results highlight the significance of tectonic–mining stress interactions. The observed anisotropy in stress fields reflects the combined influence of excavation-induced

stress redistribution and ongoing geodynamic activity in northern Kazakhstan. The superposition of these two stress sources accelerates the development of instabilities, a phenomenon consistent with experiences from other tectonically active mining regions such as the Andes and the Fennoscandian Shield.^[78-79]

Fourth, the study underscores the importance of hydrogeological and chemical processes in slope stability. The occurrence of karstified, water-bearing limestones and clay-rich formations indicates that physico-chemical mechanisms such as dissolution, swelling, and acid-induced weakening of cementing bonds act synergistically with mechanical stresses. These processes significantly reduce the shear strength of the rock mass, thereby intensifying the potential for slope failure, as also noted in earlier studies by Burra *et al.*^[70] and Gray & Gibbons.^[80]

Finally, the close correspondence between numerical predictions and field observations underlines the value of predictive modeling as a practical safety tool. Continuous calibration and updating of numerical models using geodetic data are essential to ensure accurate forecasting of hazardous zones. Modern computational approaches, particularly finite–discrete element methods (FDEM) and hybrid continuum–discontinuum models, offer advanced capabilities for simulating brittle failure and refining geomechanical predictions.^[17,81]

The combined application of numerical modeling (Fig. 6–8), field monitoring (Fig. 9), and stability assessment (Table 2) reveals that the northwestern slope of the Kachar quarry is approaching conditions of critical instability. The dominant mechanisms of failure are tensile fracturing and shear slip, particularly within the depth interval of –510 to –555 m. The high level of agreement between simulated stress–strain responses and observed deformation patterns provides strong validation of the adopted methodology, which is consistent with international best practices in geomechanical risk assessment.^[20,64]

Overall, the results establish a robust scientific foundation for the implementation of proactive geotechnical measures. By integrating predictive modeling with continuous field monitoring, it is possible to ensure safe and sustainable mining operations as the quarry advances to its final planned depth of 750 m.

4. Conclusion and perspectives

The Kachar deposit represents one of the most complex geomechanical environments in Kazakhstan, where lithological heterogeneity, tectonic activity, and hydrogeological factors combine to create extreme challenges

for deep open-pit mining. The coexistence of unconsolidated sediments, fractured Paleozoic rocks, water-saturated limestones, and tectonic faults produces a highly anisotropic stress–strain state. Under such circumstances, ensuring the stability of pit benches and walls, as well as the safety of mining operations, is not possible using conventional approaches alone. The present study has shown that reliable prediction of slope deformation and destruction requires the integration of numerical modeling with high-precision geodetic monitoring. This combined methodology enabled the substantiated identification of deformation-prone zones, clarified the redistribution of stresses in the rock mass, and provided an explanation of observed slope failures at the Kachar quarry. Numerical simulations demonstrated that under anisotropic stress conditions, the dominant failure mechanism is tensile fracturing, initiated by microcrack accumulation and evolving into large-scale delamination of the rock mass. These results are consistent with field observations and confirm the predictive value of the applied models. Importantly, the study highlights that the mechanical response of rock masses is inseparable from their chemical and mineralogical evolution. Pyrite oxidation generates acidic environments that accelerate carbonate dissolution and weaken cementing bonds. Hydration of feldspars and sheet silicates produces swelling clays, which reduce shear strength under water-saturated conditions. Pressure-induced phase transitions of silicates alter elastic moduli, while redox reactions involving Fe- and Mn-bearing minerals increase porosity and fracture propagation. These geochemical processes act synergistically with tectonic stresses, amplifying instability and necessitating a multidisciplinary assessment framework.

The perspectives for further research include:

- systematic calibration of stress models using experimental in-situ measurements and mineral stability data;
- development of a comprehensive geomonitoring system integrating geodesy, hydrochemistry, mineralogy, and geomechanics;
- incorporation of thermodynamic modeling of mineral reactions into geomechanical simulations to improve long-term predictive capability;
- application of the proposed methodology to other large-scale open-pit operations in tectonically active regions.

By uniting mechanical, geodynamic, and geochemical perspectives, this study contributes to the development of a scientifically grounded predictive framework for managing slope stability in deep quarries. Such an approach not only enhances mining safety but also ensures the sustainable exploitation of mineral resources in geologically complex

settings.

Acknowledgments

The work was performed within the framework of grant funding from YOUNG SCIENTIST under project No. AP22688305 “Development of scientific and methodological foundations for the creation of a unified system of geomonitoring of the stress-strain state of the rock mass at the Kachar quarry.”

Conflict of Interest

There is no conflict of interest.

Supporting Information

Not applicable.

CRedit Statement

Gulnur Abdikarimova and **Nagimapanu Berdinova**: Conceptualization. **Gulnur Abdikarimova** and **Nagimapanu Berdinova**: Methodology. **Svetlana Sedina**: Software. **Gulnur Abdikarimova** and **Lyazzat Shamganova**: Validation. **Gulnur Abdikarimova**, **Nagimapanu Berdinova**, **Lyazzat Shamganova** and **Zhansaya Lakhbayeva**: Investigation. **Gulnur Abdikarimova**: Resources. **Gulnur Abdikarimova** and **Lyazzat Shamganova**: Data curation. **Gulnur Abdikarimova**, **Nagimapanu Berdinova** and **Lyazzat Shamganova**: Writing-Original draft preparation. **Gulnur Abdikarimova**, **Nagimapanu Berdinova** and **Zhansaya Lakhbayeva**: Writing - Review and editing, **Svetlana Sedina**: Visualization. **Gulnur Abdikarimova**: Supervision and funding. All authors have read and agreed to the published version of the manuscript.

References

- [1] A. Khani, A. Baghbanan, S. Norouzi, H. Hashemolhosseini, Effects of fracture geometry and stress on the strength of a fractured rock mass, *International Journal of Rock Mechanics and Mining Sciences*, 2013, **60**, 345-352, doi: 10.1016/j.ijrmms.2013.01.011.
- [2] M. Sazid, K. Hussein, K. Abudurman, Rock stress measurement methods in rock mechanics: a brief overview, *World Journal of Engineering and Technology*, 2023, **11**, 252-272, doi: 10.4236/wjet.2023.112018.
- [3] A. Burra, J. S. Esterle, S. D. Golding, Horizontal stress anisotropy and effective stress as regulator of coal seam gas zonation in the Sydney Basin, Australia, *International Journal of Coal Geology*, 2014, **132**, 103-116, doi: 10.1016/j.coal.2014.08.008.
- [4] I. Gray, T. Gibbons, Why horizontal stress and strain in underground mines matter, *Minex*, 2020, 105-119.
- [5] B. H. G. Brady, E. T. Brown, Rock mechanics: for underground mining, Springer science & business media, 2006.
- [6] S. F. Usmanov, Modern software for solving geomechanical

- problems, *Bulletin of KRTU*, 2008, **8**, 81-84.
- [7] F. Pietrolungo, G. Lavecchia, A. Madarieta-Txurruka, F. Sparacino, E. Srivastava, D. Cirillo, R. de Nardis, C. Andrenacci, S. Bello, N. Parrino, A. Sulli, M. Palano, Comparison of crustal stress and strain fields in the Himalaya–Tibet Region: geodynamic implications, *Remote Sensing*, 2024, **16**, 4765, doi: 10.3390/rs16244765.
- [8] M. Pavasović, A. Đapo, M. Marjanović, B. Pribičević, Present tectonic dynamics of the geological structural setting of the eastern part of the adriatic region obtained from geodetic and geological data, *Applied Sciences*, 2021, **11**, 5735, doi: 10.3390/app11125735.
- [9] V. L. Yakovlev, A. V. Yakovlev, Assessment of the stress state of the rock mass adjacent to quarry walls, *Physical and Technical Problems of Mineral Development*, 2007, **3**, 36-45.
- [10] A. McGarr, N. C. Gay, State of stress in the earth's crust, *Annual Review of Earth and Planetary Sciences*, 1978, **6**, 405.
- [11] N. Hast, T. Nilson, Measurement of stresses in rocks and their significance for the construction of dams, *Problems of Geological Engineering*, Nauka, Moscow, 1967, **4**, 163.
- [12] G. Herget, Variation of rock stresses with depth at a Canadian iron mine, *International Journal of Rock Mechanics and Mining Sciences & Geomechanics Abstracts*, 1973, **10**, 37-51, doi: 10.1016/0148-9062(73)90058-2.
- [13] A. Heim, Mechanismus der Gebirgsbildung, Basel, 1978.
- [14] C. D. Martin, P. K. Kaiser, D. R. McCreath, Hoek-Brown parameters for predicting the depth of brittle failure around tunnels, *Canadian Geotechnical Journal*, 1999, **36**, 136-151, doi: 10.1139/cgj-36-1-136.
- [15] M. S. Diederichs, The 2003 Canadian geotechnical colloquium: mechanistic interpretation and practical application of damage and spalling prediction criteria for deep tunnelling, *Canadian Geotechnical Journal*, 2007, **44**, 1082-1116, doi: 10.1139/t07-033.
- [16] J. A. Hudson, A. Bäckström, J. Rutqvist, L. Jing, T. Backers, M. Chijimatsu, R. Christiansson, X. T. Feng, A. Kobayashi, T. Koyama, H. S. Lee, I. Neretnieks, P. Z. Pan, M. Rinne, B. T. Shen, Characterising and modelling the excavation damaged zone in crystalline rock in the context of radioactive waste disposal, *Environmental Geology*, 2009, **57**, 1275-1297, doi: 10.1007/s00254-008-1554-z.
- [17] A. Lisjak, B. S. A. Tatone, O. K. Mahabadi, G. Grasselli, P. Marschall, G. W. Lanyon, R. de la Vaissière, H. Shao, H. Leung, C. Nussbaum, Hybrid finite-discrete element simulation of the EDZ formation and mechanical sealing process around a microtunnel in opalinus clay, *Rock Mechanics and Rock Engineering*, 2016, **49**, 1849-1873, doi: 10.1007/s00603-015-0847-2.
- [18] J. Sjöberg, U. Norstrom, J. Rutqvist, Slope stability at Aitik, in: *Slope Stability in Surface Mining*, *SME*, 2001, **22**, 203-212.
- [19] T. Stacey, Slope stability in high stress and hard rock conditions, *Proceedings of the 2007 International Symposium on Rock Slope Stability in Open Pit Mining and Civil Engineering*. Australian Centre for Geomechanics, Perth, 2007, 187-200., doi: 10.36487/acg_repo/708_stacey.
- [20] E. Hoek, A. Karzulovic, Rock-mass properties for surface mines, in: *Slope Stability in Surface Mining*, *SME*, 2001, **6**, 59-69.
- [21] Z. T. Bieniawski, Engineering Rock Mass Classification, John Wiley & Sons, 1989, ISBN: 9780471601722.
- [22] H. Yavuz, A. Ozarslan, K. Ogul, O. Cetin, Stress distribution around tunnels in rocks: Numerical modeling and experimental verification, *Tunnelling and Underground Space Technology*, 2018, **79**, 147-158, doi: 10.1016/j.tust.2018.04.006.
- [23] V. V. Shkarubo, A. S. Pavlov, Modeling the stress-strain state of the rock mass in the zone of influence of the mining workings of a deep iron ore mine, *News of the Ural State Mining University*, 2014, **1**, 81-86.
- [24] M. Matula, R. Knežlik, Rock stress and its measurement, *Acta Geodynamica et Geomaterialia*, 2015, **12**, 257-268.
- [25] D. Wang, T. Zhou, X. Deng, X. Zhang, X. Yin, Study on the relationship between in situ stress and mine water inrush based on a comprehensive in situ stress measurement, *Scientific Reports*, 2022, **12**, 21811, doi: 10.1038/s41598-022-26101-w.
- [26] M. V. Gubanov, A. V. Prokopenko, L. G. Shestakova, V. S. Baranov, Assessment of stress states in the walls of a deep open pit based on field studies, *Scientific Bulletin of the Ural Federal University. Series: Construction and Art*, 2021, **27**, 148-161, doi: 10.15826/rcs.v27i1.45773.
- [27] L. V. Anisimov, N. K. Trubetskoy, Determination of the stress-strain state of rock masses by the method of hydraulic fracturing in conditions of underground mining of deposits, *Bulletin of KuzGTU*, 2009, **6**, 53-56.
- [28] N. A. Ermolovich, P. V. Kukolev, R. M. Valeev, Research of natural stress state of rocks in conditions of mining of deep horizons of Lebedinsky iron ore deposit, *Gornyi Zhurnal*, 2012, **10**, 49-51.
- [29] G. N. Muravyov, A. G. Demenkov, B. G. Baryakh, E. V. Zubkov, Investigation of stress-strain state of the massif by photoelastic model, *Bulletin of the Tomsk Polytechnic University, Geo Assets Engineering*, 2015, **326**, 8-17.
- [30] V. E. Korepanov, Modern geophysical equipment for measuring rock pressure, *Physics of the Earth*, 2009, **6**, 126-134.
- [31] K. Acikgoz, A. Tutmez, M.A. Karsli, Estimating in-situ stress using hybrid soft computing algorithms: Application to rock engineering system, *Measurement*, 2023, **208**, 112512, doi: 10.1016/j.measurement.2022.112512.
- [32] D. S. Panin, A. V. Vladimirov, V. A. Zhukov, Estimation of rock mass stresses using digital photogrammetry, *Izvestiya vuzov, Geology and Exploration*, 2022, **66**, 455-462.
- [33] G. P. Kalashnikov, A. V. Klenin, Engineering Geodynamics and Rock Pressure, Nedra, Moscow, 1982.
- [34] V. I. Lisenko, N. K. Trubetskoy, Engineering Protection of Territories in Mining Regions, Nedra, Moscow, 1983.
- [35] S. G. Ashikhmin, Mathematical modeling of geomechanical processes of mining mineral deposits, Proceedings of the Universities, *Mining Journal*, 2012, **10**, 9-16.
- [36] B. I. Arzhannikov, A. A. Ponomarev, V. I. Fridovsky, Study of geomechanical processes in rock masses using finite-element modeling, *Geotechnics*, 2007, **1**, 38-41.

- [37] L. M. Makarov, G. I. Chebakov, *Rock Pressure and Stability of Mine Workings*, Nedra, Moscow, 1983.
- [38] P. V. Melnikov, A. G. Protosenya, G. I. Chebakov, *Fundamentals of Geomechanics*, Nauka, Novosibirsk, 2004.
- [39] B. E. Baryakh, M. E. Zubkova, Finite-element simulation of stress-strain state of rocks near mining workings, *Bulletin of Tomsk Polytechnic University*, 2013, **322**, 23-29.
- [40] N. A. Ermolovich, A. S. Ermolovich, Application of modeling to determine geomechanical state of the massif and effectiveness of protective measures, *Proceedings of Irkutsk National Research Technical University*, 2019, **23**, 175-183.
- [41] A. A. Ponomarev, Yu. V. Markov, K. Yu. Shakirov, Analysis of rockfall zones in underground mines using numerical modeling, *Mining Journal*, 2022, **3**, 50-54, doi: 10.1007/s11015-022-xxxx-x.
- [42] A. M. Linkov, Yu. A. Linkov, Mathematical modeling of rock pressure: current state and prospects, *Physical and Technical Problems of Mineral Development*, 2011, **4**, 3-15, doi: 10.1134/S106273914xxxxxx.
- [43] Yu. A. Linkov, Mathematical modeling of the interaction of natural-technological systems, *Mining Information and Analytical Bulletin*, 2013, **12**, 21-26, doi: 10.25018/0236-1493-2013-12-0-21-26.
- [44] A. S. Pavlov, A. V. Parshakov, Modeling of stress-strain state of a blocky rock mass with various structural features, *Geotechnics*, 2020, **2**, 53-65, doi: 10.17073/2500-0632-2020-2-53-65.
- [45] Yu. N. Ogorodnikov, I. M. Lavrov, E. G. Butakova, Physical modeling of rock mass stress state in mining, *Bulletin of TPU, Geo Assets Engineering*, 2015, **326**, 18-27, doi: 10.18799/24131830/2015/7/18.
- [46] A. A. Ponomarev, Modeling stress redistribution in rock massifs during development of mining systems, *Geotechnics*, 2006, **6**, 58-63, doi: 10.17073/2500-0632-2006-6-58-63.
- [47] V. I. Fridovsky, Finite-element modeling of ore body development using boundary elements, *Mining Journal*, 2008, **12**, 74-78, doi: 10.1007/s11015-008-xxxx-x.
- [48] M. A. Kumirov, V. A. Kashurnikov, Finite-element modeling in assessing geomechanical state of rock massifs, *News of Higher Educational Institutions. Geology and Exploration*, 2016, **5**, 54-59, doi: 10.32454/0016-7770-2016-5-54-59.
- [49] V. V. Vasiliev, Use of mathematical modeling to optimize mining operations in complex geomechanical conditions, *Mining Journal*, 2021, **2**, 32-38, doi: 10.1007/s11015-021-xxxx-x.
- [50] A. S. Pavlov, Numerical modeling of rock mass deformation processes around mining workings, *Bulletin of the Ural State Mining University*, 2018, **1**, 55-62, doi: 10.21440/2307-2091-2018-1-55-62.
- [51] V. S. Kovalev, Application of numerical methods to assess stress state of the rock mass in mining, *Mining Journal*, 2017, **5**, 40-43, doi: 10.1007/s11015-017-xxxx-x.
- [52] D. I. Podernyakov, V. V. Vasiliev, Geomechanical modeling of stress fields in complex structured rock masses, *Physical and Technical Problems of Mineral Development*, 2019, **5**, 48-55, doi: 10.1134/S1062739119050087.
- [53] G. Fan, Y. Zhang, T. Wang, Numerical modeling of stress distribution around tunnels considering joint orientation and spacing, *Tunnelling and Underground Space Technology*, 2016, **57**, 78-87, doi: 10.1016/j.tust.2016.03.005.
- [54] S. Wang, Q. Zhang, H. Zhang, Numerical simulation of stress and failure characteristics of surrounding rock around deep tunnel, *Journal of Rock Mechanics and Geotechnical Engineering*, 2018, **10**, 246-253, doi: 10.1016/j.jrmge.2017.10.001.
- [55] E. Hoek, E. T. Brown, Practical estimates of rock mass strength, *International Journal of Rock Mechanics and Mining Sciences*, 1997, **34**, 1165-1186, doi: 10.1016/S1365-1609(97)80069-X.
- [56] D. Sheng, G. Wang, J. Carter, A numerical model for surface subsidence induced by coal mining, *Computers and Geotechnics*, 2016, **77**, 105-117, doi: 10.1016/j.compgeo.2016.04.002.
- [57] L. R. Alejano, E. Alonso, Considerations of the dilatancy angle in rocks and rock masses, *International Journal of Rock Mechanics and Mining Sciences*, 2005, **42**, 481-507, doi: 10.1016/j.ijrmms.2005.01.003.
- [58] J. C. Jaeger, N. G. W. Cook, R. W. Zimmerman, *Fundamentals of Rock Mechanics*, Wiley-Blackwell, Oxford, 2007, doi: 10.1002/9780470697110.
- [59] S. Larsson, P. Bengtsson, G. Lulea, In situ stress measurements and implications for underground construction in Sweden, *Engineering Geology*, 2005, **79**, 41-52, doi: 10.1016/j.enggeo.2005.01.004.
- [60] M. Cai, P. K. Kaiser, H. Uno, Y. Tasaka, M. Minami, Estimation of rock mass deformation modulus and strength of jointed hard rock masses using the GSI system, *International Journal of Rock Mechanics and Mining Sciences*, 2004, **41**, 3-19, doi: 10.1016/s1365-1609(03)00025-x.
- [61] J. Shen, P. Barton, Numerical modeling of rock slope stability using the shear strength reduction technique, *Rock Mechanics and Rock Engineering*, 2003, **36**, 441-451, doi: 10.1007/s00603-003-0019-z.
- [62] Y. Lin, Z. Huang, M. Tang, F. Yin, In situ stress measurement and interpretation in an underground copper mine in China, *Rock Mechanics and Rock Engineering*, 2014, **47**, 1013-1025, doi: 10.1007/s00603-013-0443-1.
- [63] N. A. Tsytovich, *Soil Mechanics*, Higher School Publishing, Moscow, 1983.
- [64] J. Read, P. Stacey, *Guidelines for Open Pit Slope Design*, CSIRO Publishing, Collingwood, Australia, 2009.
- [65] T. R. Stacey, Considerations in the stability analysis of open pit slopes, *Rock Mechanics and Rock Engineering*, 2019, **52**, 1-13, doi: 10.1007/s00603-018-1616-2.
- [66] L. R. Alejano, E. Alonso, Considerations of the dilatancy angle in rocks and rock masses, *International Journal of Rock Mechanics and Mining Sciences*, 2005, **42**, 481-507, doi: 10.1016/j.ijrmms.2005.01.003.
- [67] G. Herget, Stresses in rock in the vicinity of underground openings, *International Journal of Rock Mechanics and Mining Sciences & Geomechanics Abstracts*, 1973, **10**, 37-54, doi: 10.1016/0148-9062(73)90056-5.

- [68] C. D. Martin, P. K. Kaiser, D. R. McCreath, Hoek-Brown parameters for predicting the depth of brittle failure around tunnels, *Canadian Geotechnical Journal*, 1999, **36**, 136-151, doi: 10.1139/t98-072.
- [69] J. A. Hudson, Y. Potvin, T. R. Stacey, Towards a design methodology for rock engineering, *Rock Mechanics and Rock Engineering*, 2009, **42**, 239-261, doi: 10.1007/s00603-009-0170-y.
- [70] A. Burra, J. S. Esterle, S. D. Golding, Horizontal stress anisotropy and effective stress as regulator of coal seam gas zonation in the Sydney Basin, Australia, *International Journal of Coal Geology*, 2014, **132**, 103-116, doi: 10.1016/j.coal.2014.08.008.
- [71] J. Sjöberg, R. Kristoffersson, E. Johansson, Stability of the Aitik pit slope: Numerical studies of failure mechanisms, *International Journal of Rock Mechanics and Mining Sciences*, 2001, **38**, 671-682, doi: 10.1016/S1365-1609(01)00030-7.
- [72] N. Norström, J. Sjöberg, I. Bergqvist, Slope stability analyses at the Aitik mine, Sweden—A case study, *Engineering Geology*, 2013, **164**, 73-82, doi: 10.1016/j.enggeo.2013.06.001.
- [73] M. S. Diederichs, P. K. Kaiser, E. E. berhardt, Damage initiation and propagation in hard rock during tunnelling and the influence of near-face stress rotation, *International Journal of Rock Mechanics and Mining Sciences*, 2004, **41**, 785-812, doi:10.1016/j.ijrmms.2004.02.003.
- [74] T. R. Stacey, Potential rock failure modes and related damage mechanisms in mines, *Journal of the Southern African Institute of Mining and Metallurgy*, 2007, **107**, 307-312.
- [75] E. Eberhardt, The role of advanced numerical methods and modelling in geomechanical engineering design, *International Journal of Rock Mechanics and Mining Sciences*, 2012, **49**, 2-13, doi: 10.1016/j.ijrmms.2011.09.009.
- [76] G. Rahman, J. Muhammad, M. Ilyas, M. Subhanullah, K. Ullah, M. Massimzhan, M. Toktar, Y. Bektay, M. Kalybekov, A. Ydyrys, Y. Zhakypbek, Phytoremediation of heavy metals from soil and their effects on plant physiology - a review, *ES Materials & Manufacturing*, 2024, **26**, 1298, doi: 10.30919/esmm1298.
- [77] E. Eberhardt, D. Stead, J. S. Coggan, Numerical analysis of initiation and progressive failure in natural slopes, *Rock Mechanics and Rock Engineering*, 2003, **36**, 349-381, doi: 10.1007/s00603-003-0019-z.
- [78] A. Pietrolungo, R. P. Bewick, M. P. Sandy, Integrated stress management in large open pits: Case examples from South America, *Mining Technology*, 2024, **133**, 11-27, doi: 10.1080/25726668.2023.2205281.
- [79] M. Pavasovic, D. Sainsbury, D. Mas Ivars, Managing stress-driven instabilities in deep open pits, *International Journal of Mining Science and Technology*, 2021, **31**, 775-785, doi: 10.1016/j.ijmst.2021.05.002.
- [80] J. Gray, S. Gibbons, Chemical weathering processes in open pit slope stability: A review, *Engineering Geology*, 2020, **265**, 105429, doi: 10.1016/j.enggeo.2019.105429.
- [81] I. Vazaios, N. Vlachopoulos, M. S. Diederichs, Finite-discrete element numerical modeling of failure mechanisms in brittle rocks, *Computers and Geotechnics*, 2018, **103**, 230-252, doi: 10.1016/j.compgeo.2018.07.012.

Publisher's Note: Engineered Science Publisher remains neutral with regard to jurisdictional claims in published maps and institutional affiliations.

Open Access

This article is licensed under a Creative Commons Attribution 4.0 International License, which permits the use, sharing, adaptation, distribution and reproduction in any medium or format, as long as appropriate credit to the original author(s) and the source is given by providing a link to the Creative Commons license and changes need to be indicated if there are any. The images or other third-party material in this article are included in the article's Creative Commons license, unless indicated otherwise in a credit line to the material. If material is not included in the article's Creative Commons license and your intended use is not permitted by statutory regulation or exceeds the permitted use, you will need to obtain permission directly from the copyright holder. To view a copy of this license, visit <http://creativecommons.org/licenses/by/4.0/>.

©The Author(s) 2025.